Appendix B: AIGKC Fishery CPUE Standardization

Tyler Jackson
Alaska Department of Fish and Game, tyler.jackson@alaska.gov

May 2025

Background

The AIGKC stock assessment has used catch per unit effort (CPUE) data collected by at-sea observers and fish ticket data as a primary index of stock abundance since model development began (Siddeek et al. 2017; Siddeek et al. 2016). Standardized indices are estimated for three periods: 1) fish ticket CPUE from 1985 - 1998, 2) observer CPUE during the pre-rationalized period (1995 - 2004), and 3) observer CPUE during the post-rationalized period (2005 - 2023). This appendix details updates to the CPUE standardization process for the the post-rationalized period for which there is new observer data. It also includes explorations of CPUE standardization using spatiotemporal models to be further evaluated during the next assessment cycle.

Post-Rationalized CPUE Index

Major Changes

The only changes in CPUE standardization relative to the 2024 final assessment is the addition of observer data collected during the 2024/25 season.

Methods

Core Data Preparation

Observer data sets were limited to pots that represented core fishing effort in an attempt to remove observations that may not be indicative of overall fishing performance. Core vessels and permit holders during the pre-rationalized time series were those that participated in more than a single season. The fleet was consolidated enough in the post-rationalized time series that reductions on number of vessels and permit holders were not warranted. Following Siddeek et al. (2016; 2023) several gear types were combined, and pot types not typical to the directed fishery were removed. Since many fishing seasons in the pre-rationalized era did not align with the crab year used in the post-rationalized era (July - June), crab year was assigned to pre-2005 data *post hoc*. Observer pots sampled on dates that fall after June 30 in a given season were assigned the next crab year (Siddeek et al. 2016, 2023). Soak time and depth data were truncated by removing the outer 5% and 1% of distributions, respectively.

Model Fitting

CPUE standardization models were fit using general additive models (GAM) as implemented in the R package *mgcv* (Wood 2004). Negative binomial and Tweedie error distributions with a log link were evaluated

during the 2024 final assessment (Jackson 2024 Appendix A). Negative binomial GAMs performed best for the pre-rationalized period, while Tweedie GAMs performed better for the post-rationalized period. Since this analysis only updates the standardization of post-rationalized CPUE data, only Tweedie models were considered. The power variable, p, that relates the Tweedie mean to its variance was estimated as a model parameter. All splines were fit as thin plate regression splines, with smoothness determined by generalized cross-validation (Wood 2004).

Variable Selection

Null models included only crab year as an explanatory variable

$$\ln(CPUE_i) = Year_{y,i} \tag{1}$$

The full scope of models evaluated included gear (i.e., pot size), vessel, permit holder (i.e., proxy for captain), month and block (i.e., discrete geographic subarea, Figure 1) as factorial variables. Prospective smoothed terms include soak time, depth, and slope angle. Sea floor slope angle (degrees) was computed in ArcGIS (Redlands 2011) from a 100-m resolution raster surface of Aleutian Islands bathymetry (Zimmermann 2013). Addition of new variables was considered significant if AIC decreased by at least two per degree of freedom lost and R^2 increased by at least 0.01. Variables were added (or subtracted) from the model until no candidate variables met AIC and R^2 criteria. Consistent AIC (CAIC; -2LogLik+(ln(n)+1)p; Bozdogan 1987) was used instead of the traditional AIC, in which n is the number of observations and p is the number of parameters (Siddeek et al. 2016, 2023). If forward and backward selection produced conflicting results, the best model was determined by CAIC.

$$R^2 = \frac{D_{Null} - D_{Resid}}{D_{Null}} \tag{2}$$

Model Diagnostics

Simulated residuals were calculated using the R package $DHARMa$ (Hartig 2020). $DHARMa$ simulates a cumulative density function for each observation of the response variable for the fitted model and computes the residual as the value of the empirical density function at the value of the observed data. Residuals are standardized from 0 to 1 and distributed uniformly if the model is correctly specified.

Partial effects were plotted to view the relationship between CPUE and individual variables. Step plots that show the change the standardized index with addition of each explanatory variable were also examined to consider the influence of each variable (Bishop et al. 2008; Bentley et al. 2012).

CPUE index

Following Siddeek et al. (2016, 2023) standardized CPUE index was extracted from the models as the year coefficient (β_i) with the first level set to zero and scaled to canonical coefficients (β'_i) as

$$\beta'_i = \frac{\beta_i}{\bar{\beta}} \tag{3}$$

where

$$\bar{\beta} = \sqrt[n_j]{\prod_{j=1}^{n_j} \beta_{i,j}} \tag{4}$$

and n_j is the number of levels in the year variable. Nominal CPUE was scaled by the same method for comparison.

Results

Forward and backward selection resulted in different 'best' models in both subdistricts. The best forward selection model in the EAG included (in addition to year) vessel, permit holder, gear type, and soak time, whereas backwards selection did not include permit holder (Table 2). The backward selection model was chosen for index standardization (Δ AIC = -46). In the WAG, forward selection resulted in a model including vessel, gear type, and month, whereas backward selection included permit holder instead of month and was used for index standardization (Δ AIC = -38) (Table 3). Residual diagnostics did not indicate misspecification in best models for either subdistrict (Figure 2 and 3).

Standardized indices differed minimally from null model indices. Vessel and permit holder appeared to have the largest influence on the resulting index in the EAG and WAG, respectively (Figure6 and 7). Standardized indices track nominal indices, as expected. Relative to the 2023/4, both subdistricts underwent a decrease in CPUE (Figure 8).

Spatiotemporal GAMM

Several efforts have been made to account for spatial and spatiotemporal variability in fishing effort and CPUE including specifying large-scale blocks within subdistricts (here; Siddeek et al. 2016), interactions between blocks and year (Jackson 2024, Siddeek et al. 2023), non-parametric smooths of latitude and longitude, and interactions between year and smooth terms (Jackson 2024). Geostatistical models may provide better utility over previous approaches given their ability to estimate spatial correlations and account for varying spatial coverage (Maunder et al. 2020).

Methods

Data Preparation

Core observer data preparation was the same as used for the 2025 final assessment CPUE standardization, with some minor changes to gear types included. Pot sizes 4'x4', 10'x10', 8'x8' (EAG only), and 6.5'x7' (WAG only) were removed due to small sample sizes. Pot locations were transforms to UTM coordinates using zone 2N.

GAMM

Saptiotemporal GAMMs were constructed using the R package *sdmTMB* and *sdmTMBextra* (R Core Team 2024; Anderson et al., 2024; Anderson et al., 2025). This approach models spatial random effects as a series of Gaussian random fields, which are approximated using stochastic partial differential equation matrices (SPDE) (Lindgren et al., 2011). Correlation of spatial random effects is constrained by the Matérn covariance function (Anderson et al., 2022).

The underlying spatial domain of the model was represented by a triangular mesh constructed using k-means clustering with 150 knots. Spatial polygons of the Aleutian Islands were downloaded using the R package *geodata* (Hijmans et al., 2025) and used as barriers to spatial correlation within the mesh. Mesh construction was not rigorously evaluated for these explorations and should be revisited in future analyses.

In addition to year, gear type was included as a factor covariate, soak time and depth were included as smooth splines as described above, and vessel was included as a random effect. Since soak times have increased over time as the fishery has become consolidated and competition has decreased, models with a

soak time:year interaction were also evaluated. Models assumed a Tweedie error distribution with log link function and estimated power variable, p. Spatiotemporal random fields were modeled as independent and identically distributed process. Pre- and post-rationalization periods were fit in a single model to 1) leverage the most available data within the standardization model, and 2) avoid fitting two non-overlapping indices in the assessment model (Hoyle et al., 2024).

Model Diagnostics

Model diagnosis utilized $DHARMa$ residuals following the approach described above. Several other diagnostics including tests of convergence and range of parameter estimates are built in to $sdmTMB$. Differences between observed and fitted values were also plotted over the spatial domain to identify any patterns.

Index Prediction

Standardized CPUE index was estimated by constructing a prediction data set based on vertices of the model mesh. Soak time and depth were set to mean values, while gear type and vessel were set to mode values. Predictions were summed across the spatial domain using area weighting. Annual estimates were then scaled to canonical coefficients as described above.

Results and Conclusions

Full models successfully converged and DHARMa residuals did not identify misspecifications. The EAG model with a soak time by year interaction converged, but flagged large standard errors associated with smooth terms (i.e., soak time). The WAG model with soak time year interaction did not converge, and should be further explored over the next assessment cycle.

The effect of gear type suggested increasing CPUE with large pots and considerably lower CPUE for round pots (Figures 12 and 18). Smoothed soak time was approximately dome shaped for both subdistricts, though when fit using an interaction with year in the EAG, the relationship was weak and linear in most years (Figure 13). Spatial and spatiotemporal random effects are shown in Figures 14 and 19, and 15 and 20, respectively. Maps of predicted CPUE indicated that in years with higher CPUE, estimated CPUE was higher across the full model domain, not just the areas with data (Figures 16 and 21). Standard errors on predictions suggested uncertainty is highest around the outside of the mesh, but not necessarily greater among mesh triangles with fewer or no data (Figure 17 and 22).

Adding vessel as a random effect and smoothed soak time had the greatest impact on the standardized index in both subdistricts (Figures 23 and 25). Ultimately, standardized indices were greater than nominal indices during pre-rationalized years, and less than nominal indices during post-rationalized years. Indices resulting from spatiotemporal GAMMs followed similar trajectories to indices derived from a non-spatial GAMM (Figures 24 and 26).

Spatiotemporal models seem suitable for standardization of AIGKC CPUE data given clear spatial variability in the fishery footprint, though resulting indices were not drastically different than those estimated from simpler models. These models should be revisited during the September 2025 meeting, with alternative model scenarios that include the resulting CPUE index.

Tables

Table 1: Total sample size and number of levels for each factor covariate by time period and subdistrict through the 2024/25 season.

	EAG	WAG
N	10,514	18,060
Permit Holder	16	18
Vessel	9	7
Gear	4	7
Block	4	6
Month	8	10

Table 2: Residual degrees of freedom, AIC, and R^2 for the EAG post-rationalized period best legal CPUE model including year (Yr), vessel (Ves), gear type (Gr), and s(soak time).

Form ($p = 1.384$)	Residual DF (Δ DF)	AIC (Δ AIC)	R^2 (Δ R^2)
Yr + s(soak time, 4.44) + Mon + Ves + Gr	10,471.56	91,962	0.14
+ s(depth)	-3.81	15.13	0.002
+ s(slope)	-2.89	7.70	0.002
+ Block	-3.00	23.01	0.001
- Permit Holder	-12.5	46	0.006

Table 3: Residual degrees of freedom, AIC, and R^2 for the WAG post-rationalized period best legal CPUE model including year (Yr), gear type (Gr), permit holder (PH), and s(longitude, latitude).

Form ($p = 1.495$)	Residual DF (Δ DF)	AIC (Δ AIC)	R^2 (Δ R^2)
Yr + Mo + PH + Gr	17,008	142,306	0.099
+ s(soak time)	-8.03	-30.95	0.005
+ s(depth)	-4.20	-32.96	0.003
+ s(slope)	-2.97	4.48	0.001
+ Block	-5.00	14.28	0.002
- Vessel	-2	-14.9	0.000

Table 4: Standardized observer CPUE index and associated standard errors for the post-rationalized period in the EAG and WAG.

	multicolumn2cEAG	multicolumn2cWAG		
Year	Index	σ	Index	σ
2005	1.021	0.03	1.194	0.03
2006	0.749	0.03	1.208	0.03
2007	0.850	0.02	1.201	0.04
2008	0.876	0.03	1.347	0.03
2009	0.726	0.04	1.441	0.03
2010	0.713	0.03	1.200	0.03
2011	1.043	0.03	1.263	0.03
2012	0.997	0.03	1.290	0.03
2013	0.977	0.03	0.911	0.03
2014	1.249	0.03	0.873	0.03
2015	1.282	0.03	0.833	0.03
2016	1.035	0.03	0.929	0.03
2017	1.000	0.03	0.993	0.03
2018	1.182	0.03	1.226	0.03
2019	1.113	0.03	0.972	0.03
2020	1.005	0.03	0.910	0.03
2021	0.916	0.03	0.718	0.03
2022	1.238	0.04	0.686	0.04
2023	1.234	0.03	0.771	0.04
2024	1.088	0.03	0.604	0.06

Figures

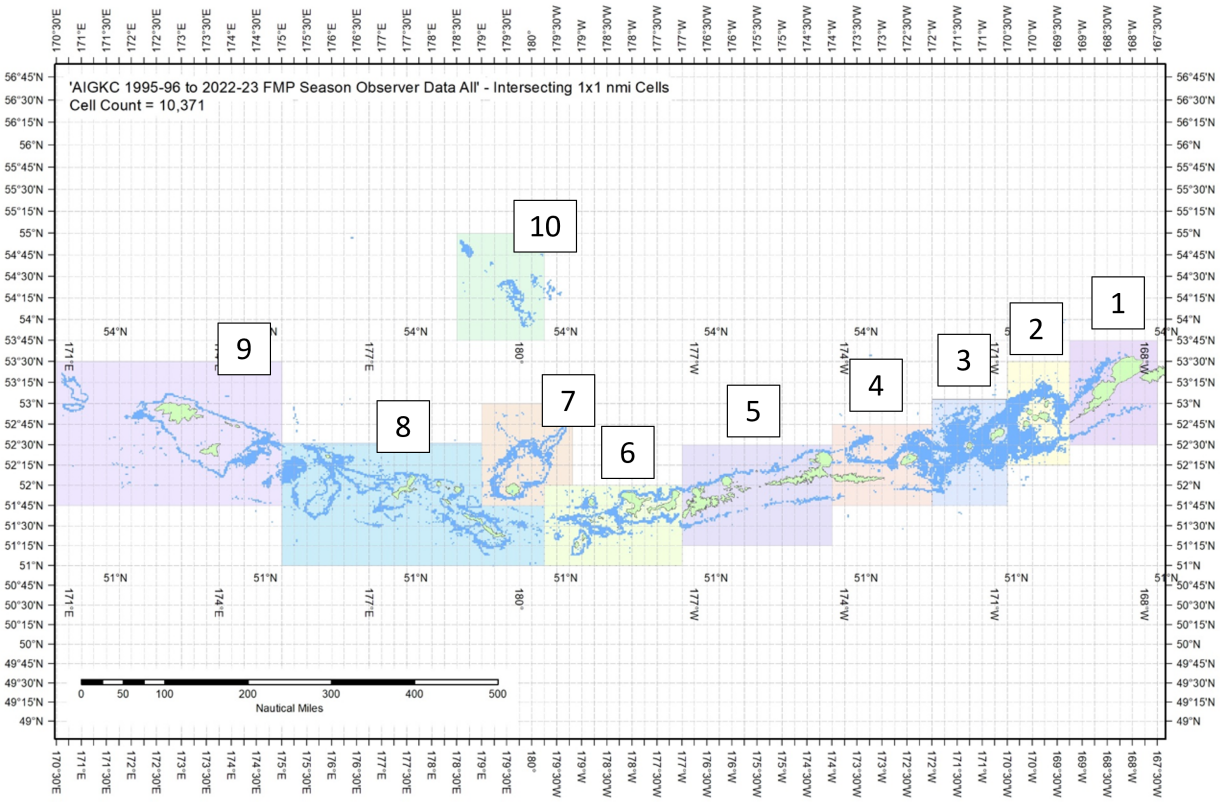

Figure 1: The 1995/96-2022/23 AIGKC observer pot samples enmeshed in 10 blocks.

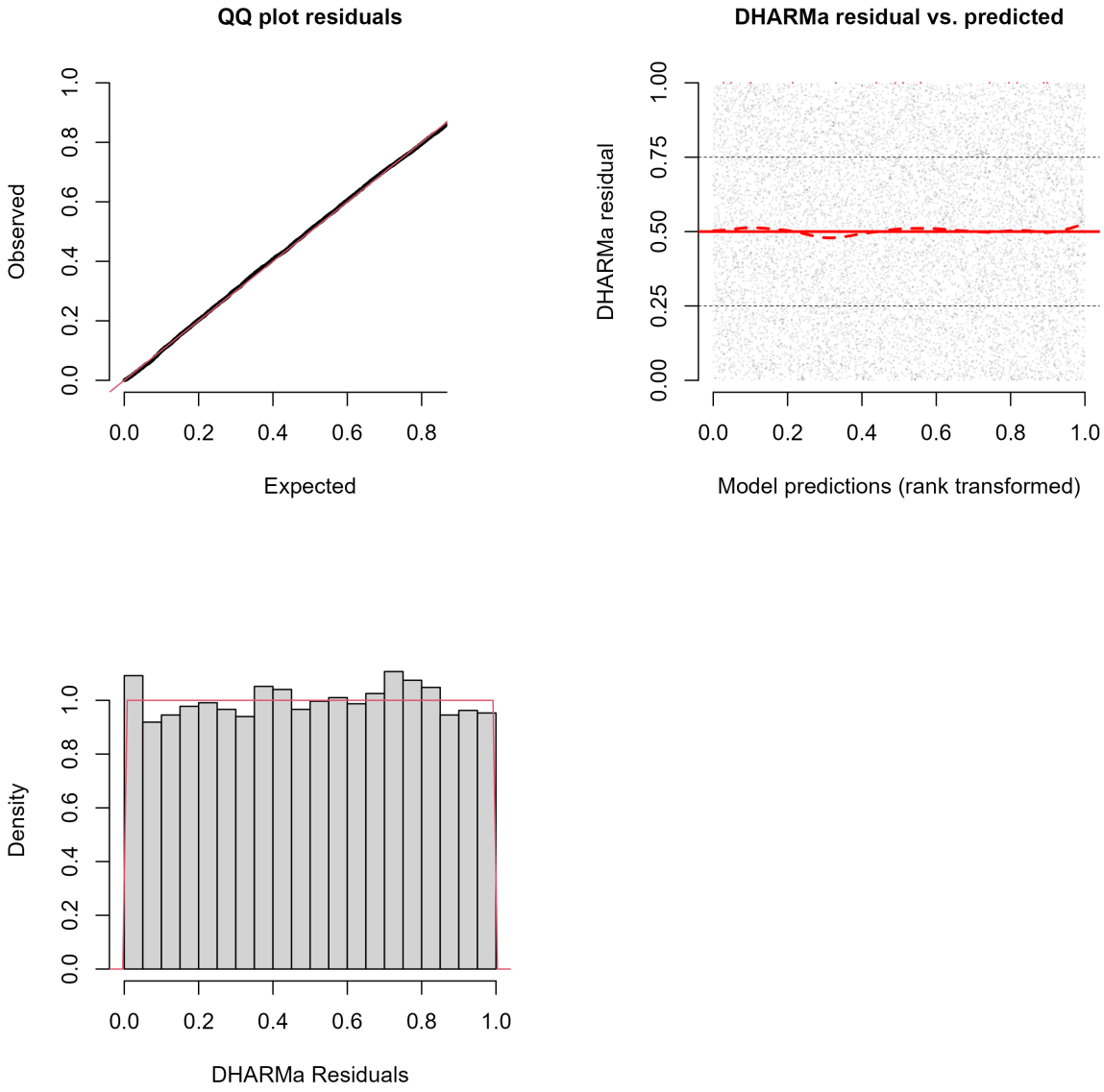

Figure 2: DHARMa residual plots for the final Tweedie GAM fit to legal CPUE during the post-rationalized period in the EAG.

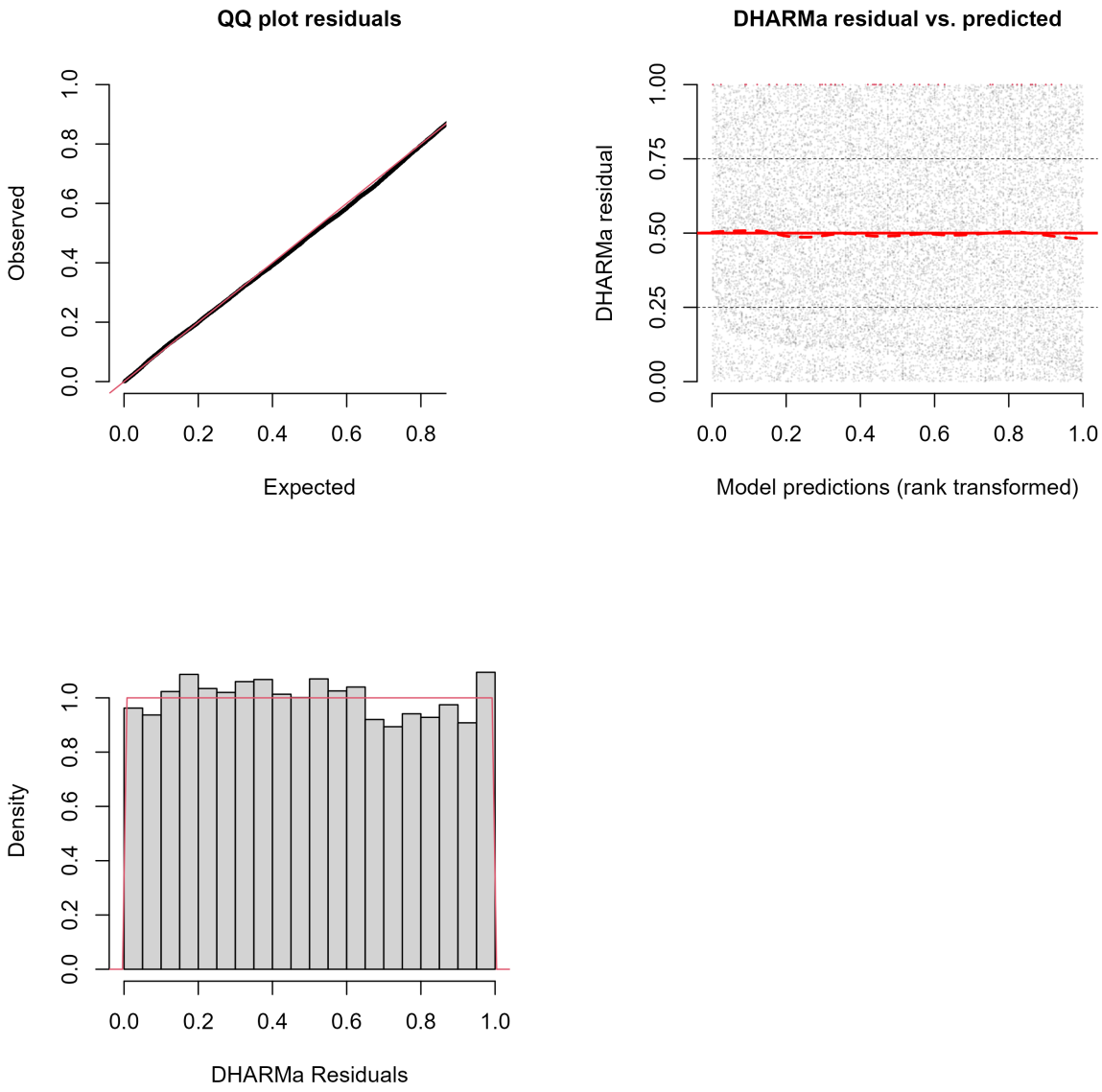

Figure 3: DHARMa residual plots for the final Tweedie GAM fit to legal CPUE during the post-rationalized period in the WAG.

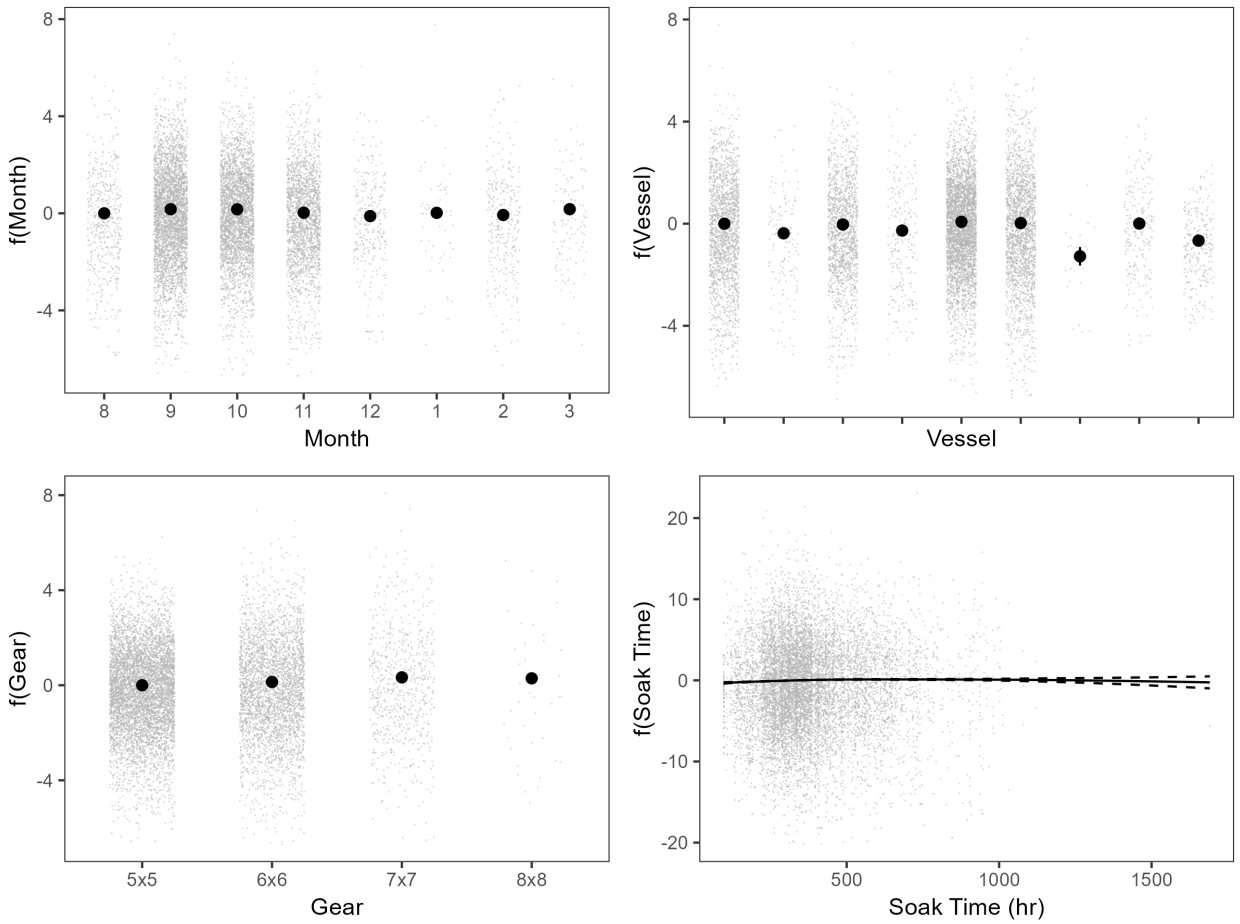

Figure 4: Marginal effects of month, permit holder, and gear type with associated partial residuals for the final model fit to legal CPUE during the post-rationalized period in the EAG.

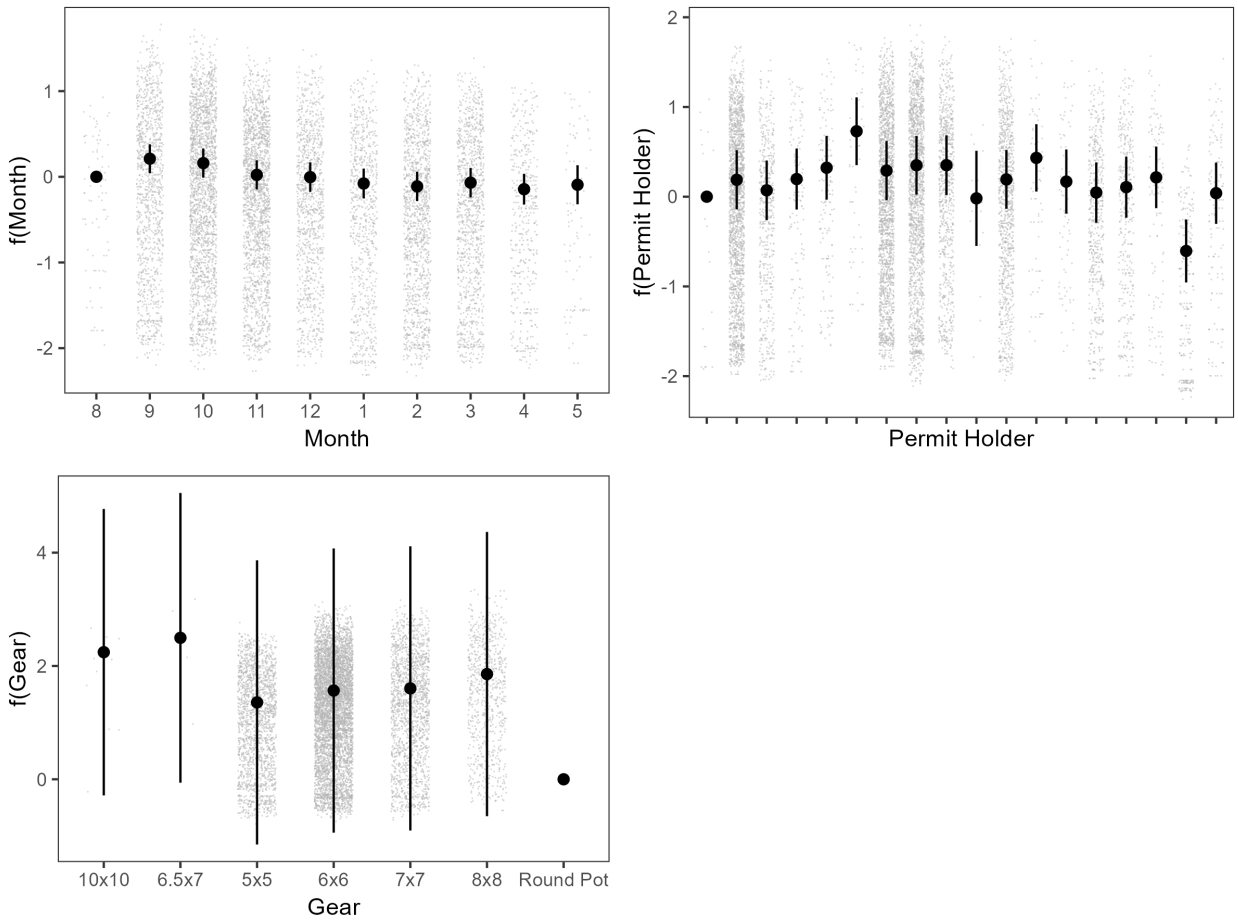

Figure 5: Marginal effects of month, permit holder, and gear type with associated partial residuals for the final model fit to legal CPUE during the post-rationalized period in the WAG.

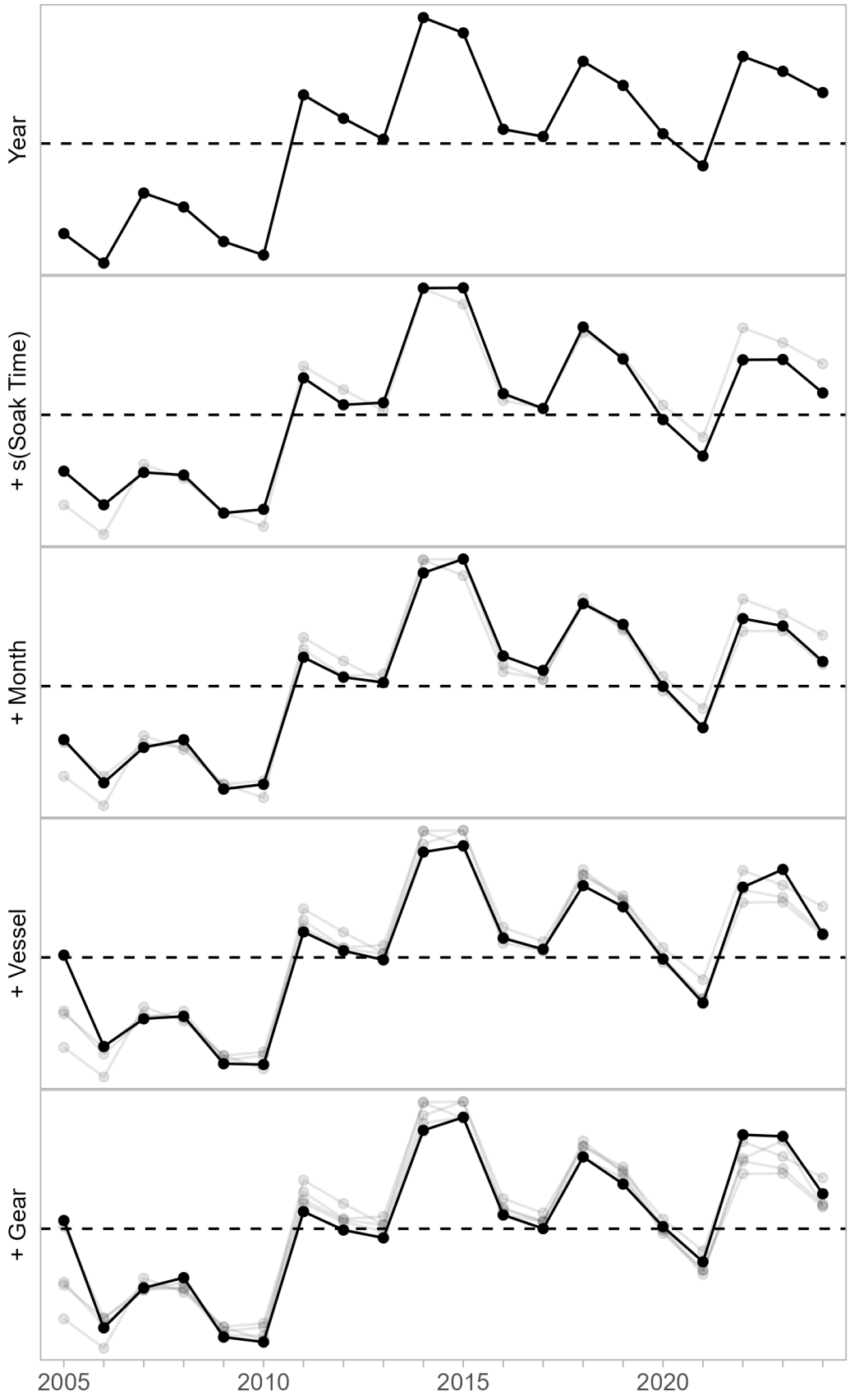

Figure 6: Step plot of CPUE index for the final model fit to legal CPUE during the post-rationalized period in the EAG.

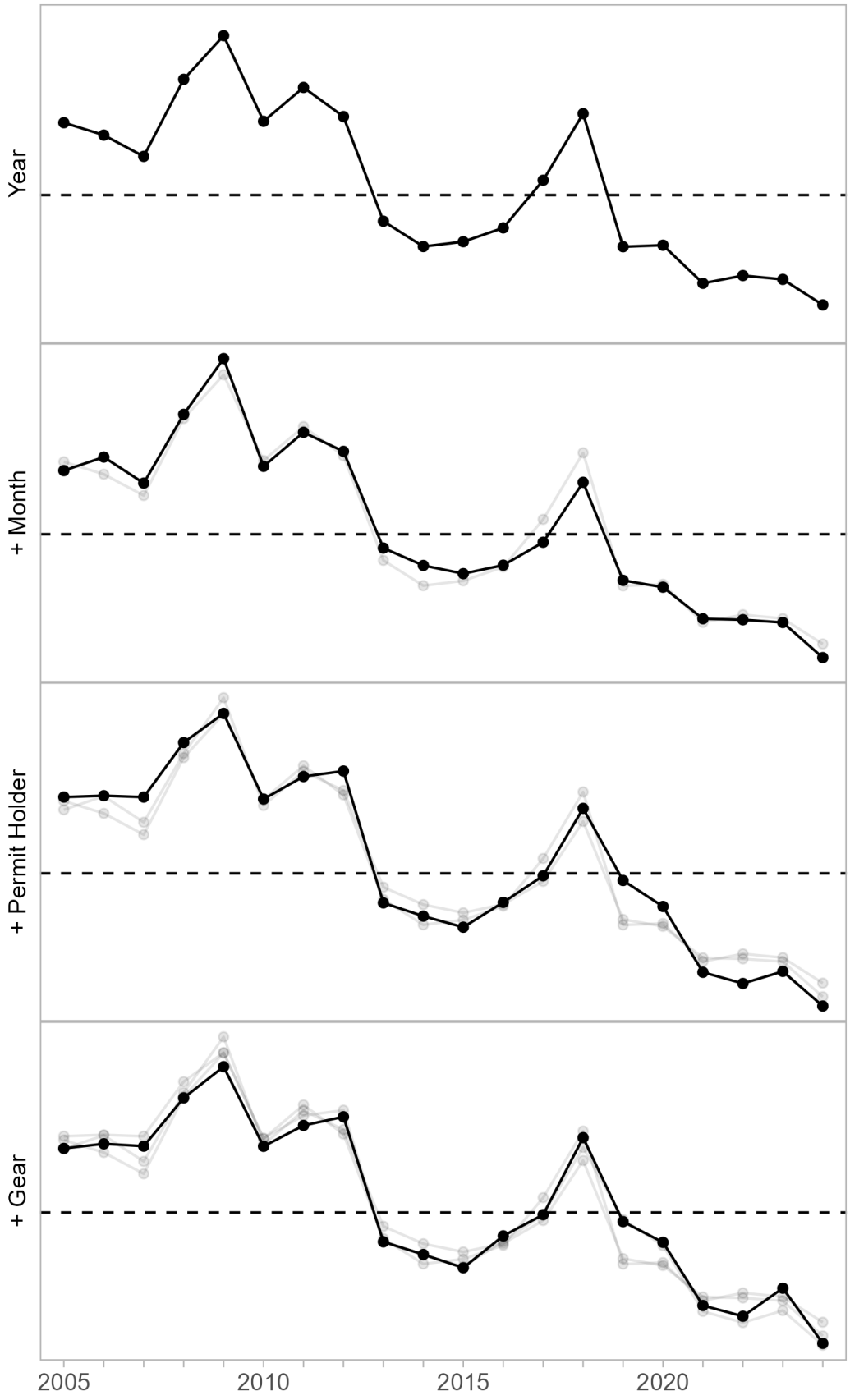

Figure 7: Step plot of CPUE index for the final model fit to legal CPUE during the post-rationalized period in the WAG.

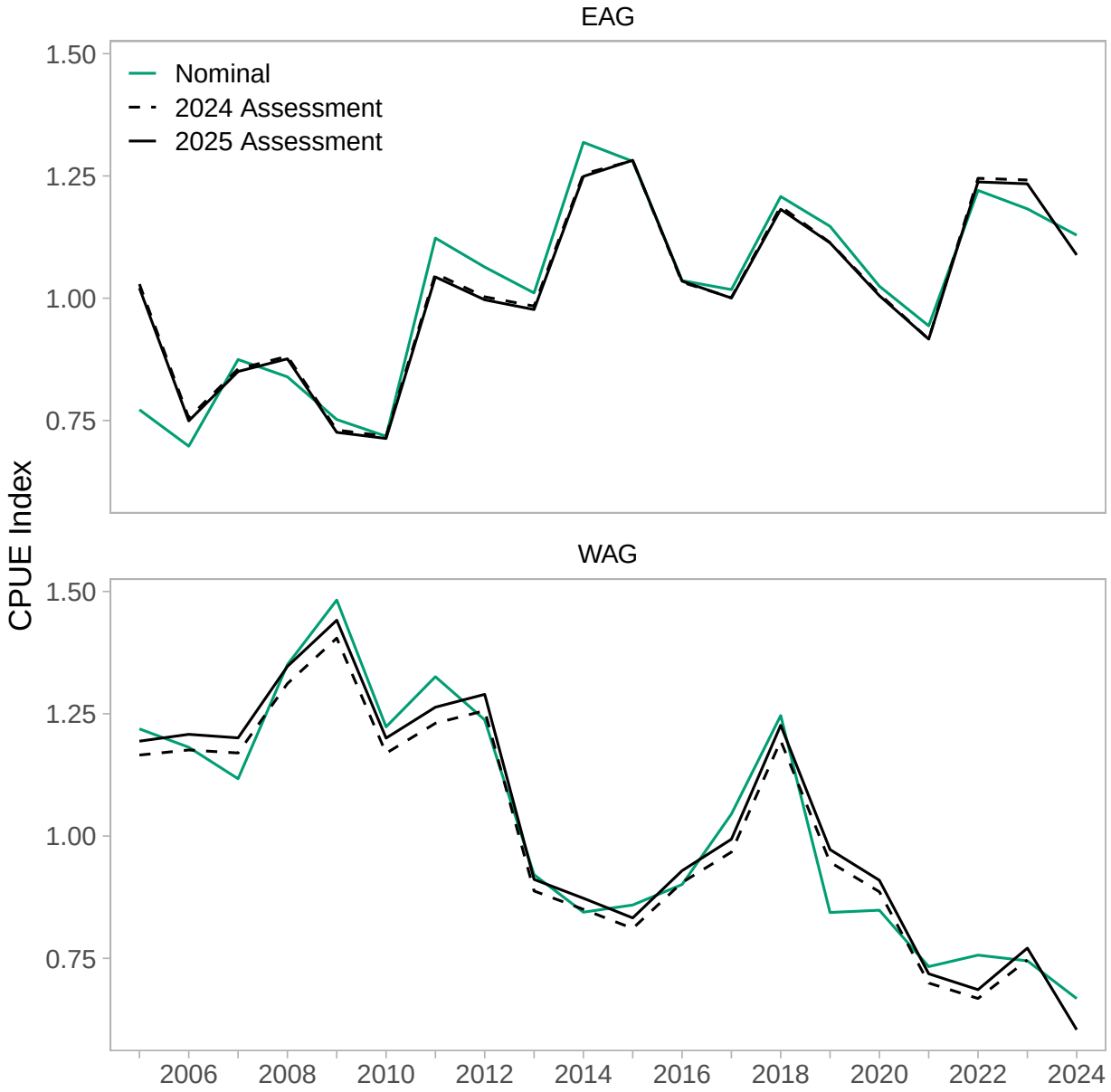

Figure 8: Step plot of CPUE index for the final model fit to legal CPUE during the post-rationalized period in the WAG.

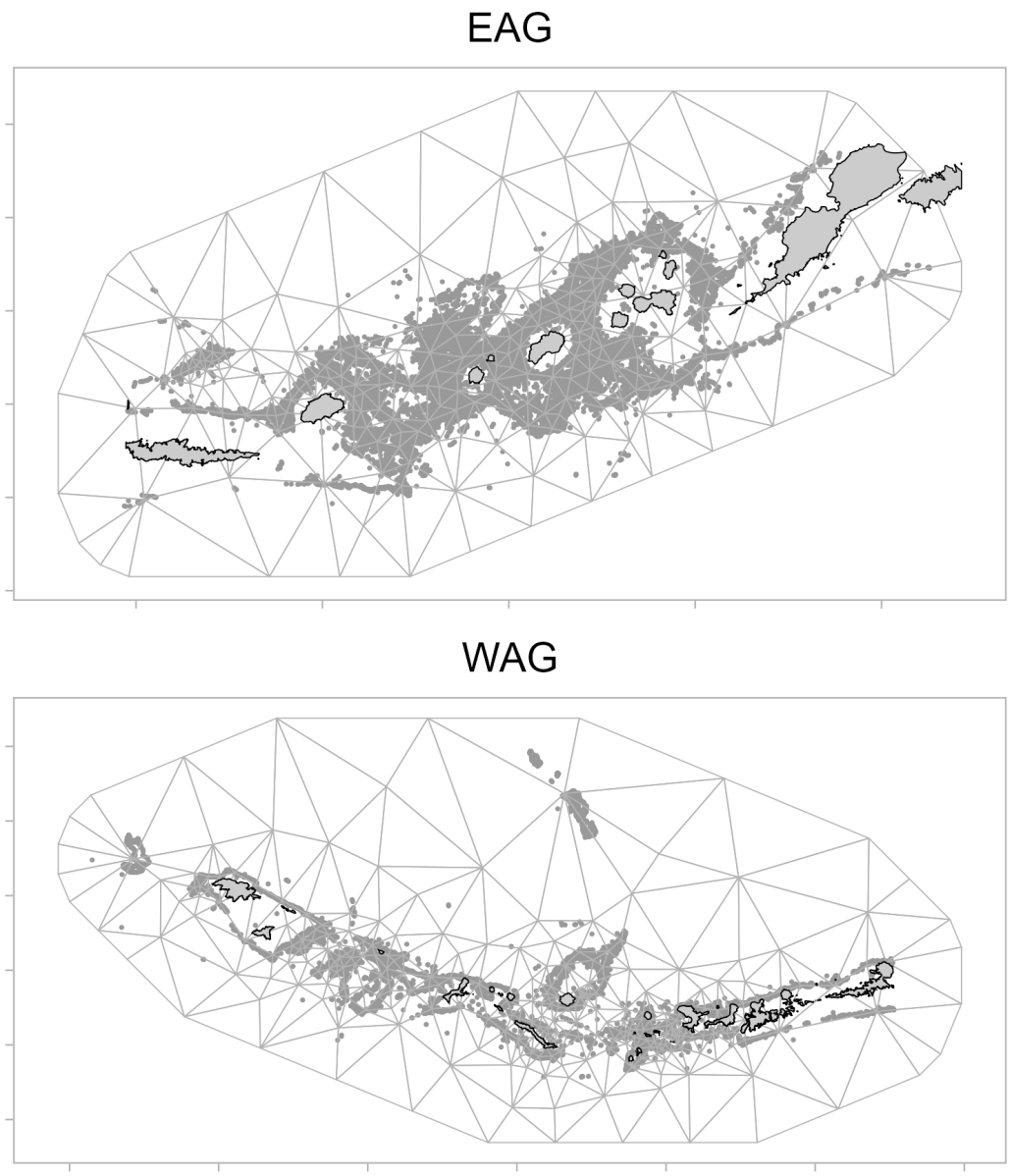

Figure 9: Triangular mesh based on k-means clustering with 150 knots used in spatiotemporal GAMMs for EAG and WAG. Grey points are observer pot locations.

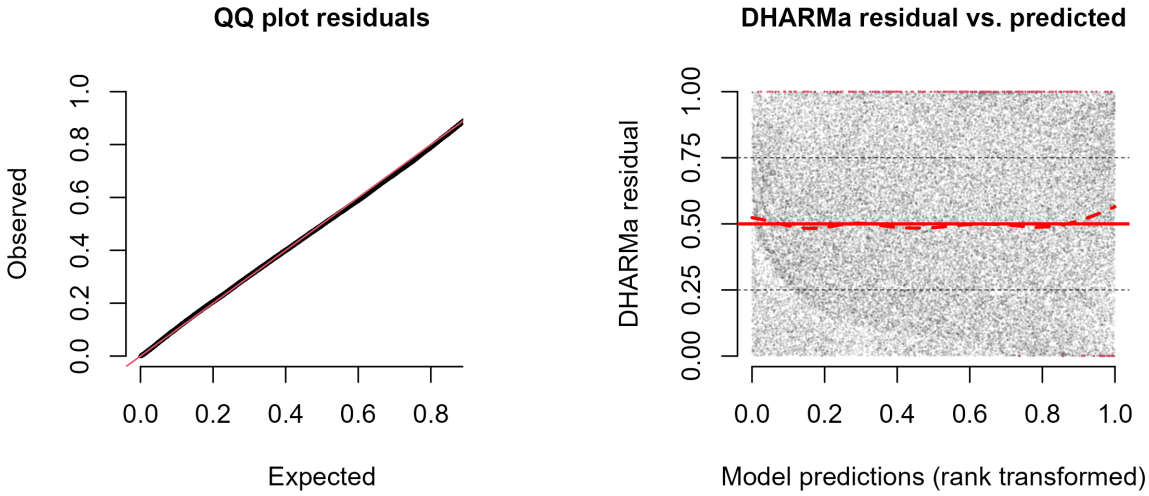

Figure 10: DHARMa residual plots for the final Tweedie spatiotemporal GAMM fit to legal CPUE in the EAG.

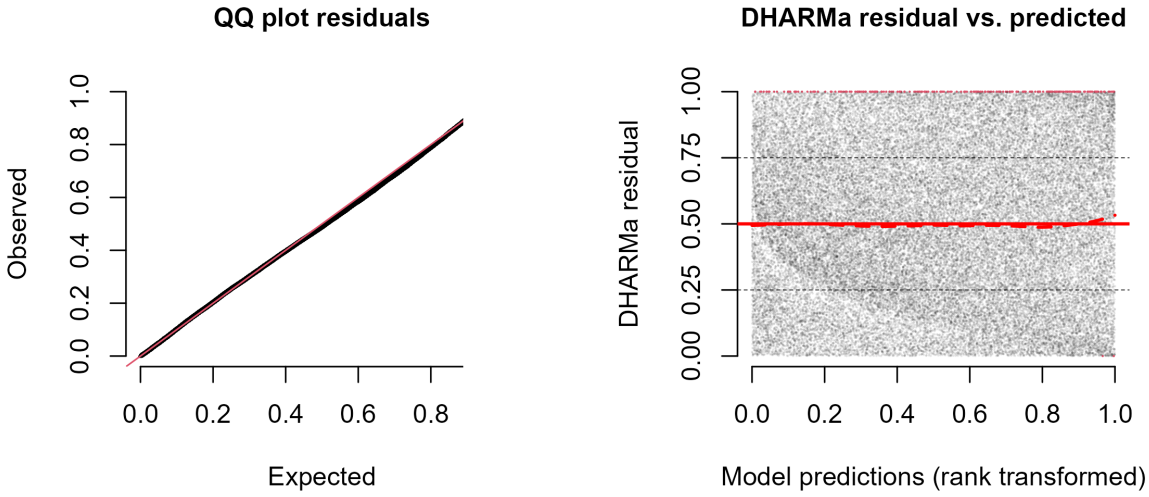

Figure 11: DHARMa residual plots for the final Tweedie spatiotemporal GAMM fit to legal CPUE in the WAG.

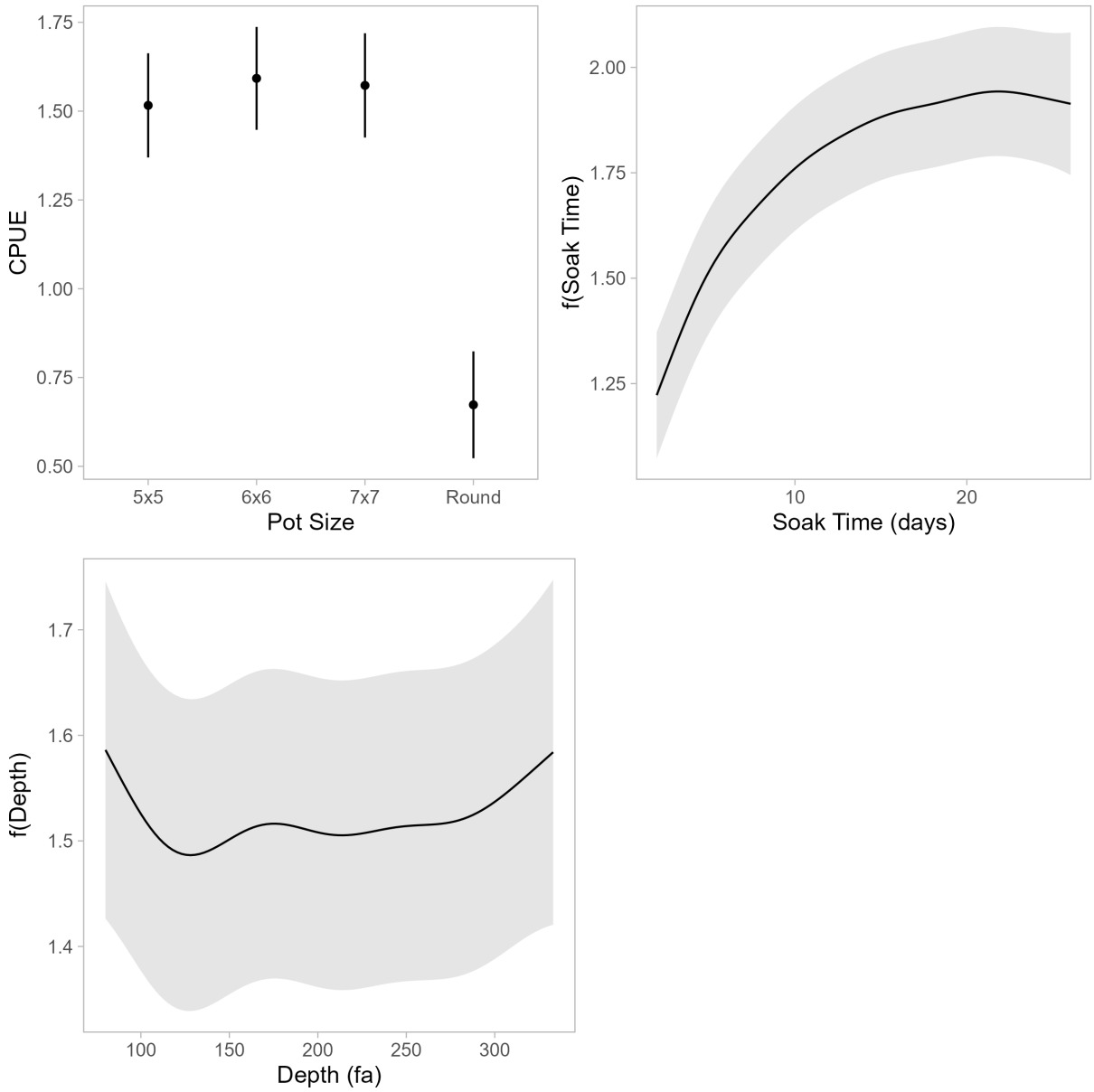

Figure 12: Marginal effects of gear type, soak time, and depth for the spatiotemporal model fit to the EAG.

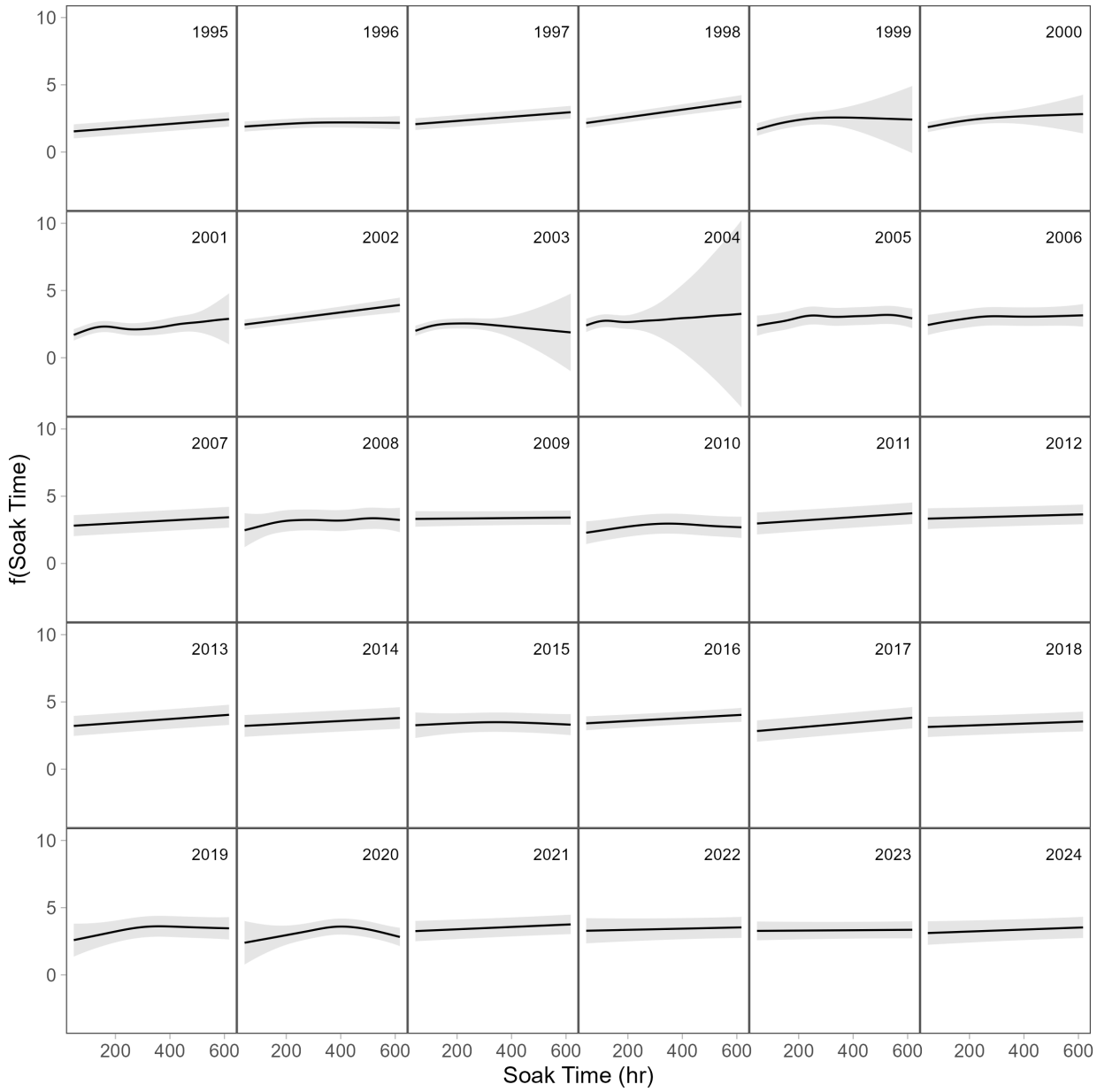

Figure 13: Marginal effect of the interaction between soak time and year for the spatiotemporal model fit to the EAG.

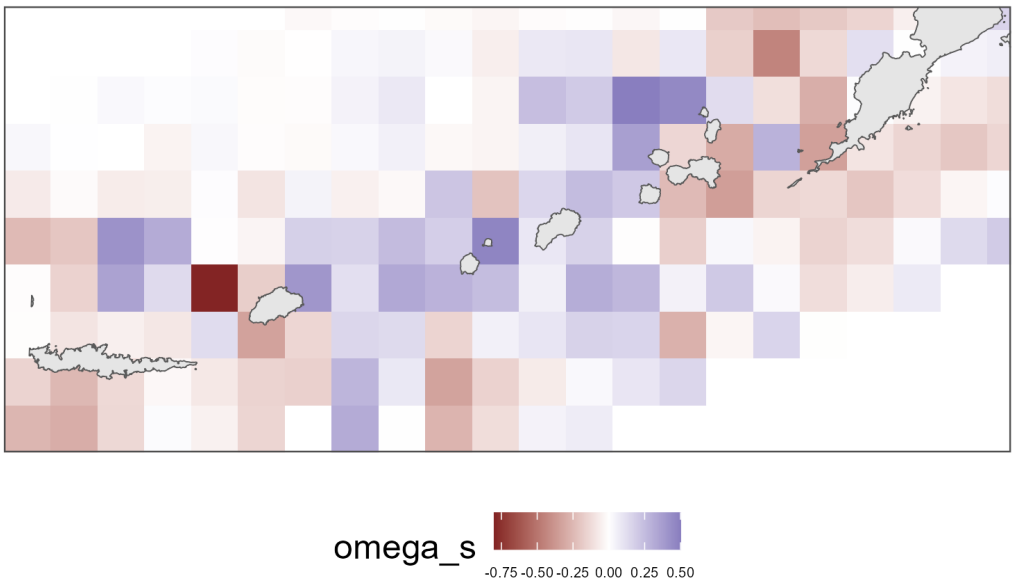

Figure 14: Spatial random effect for the spatiotemporal model fit to the EAG.

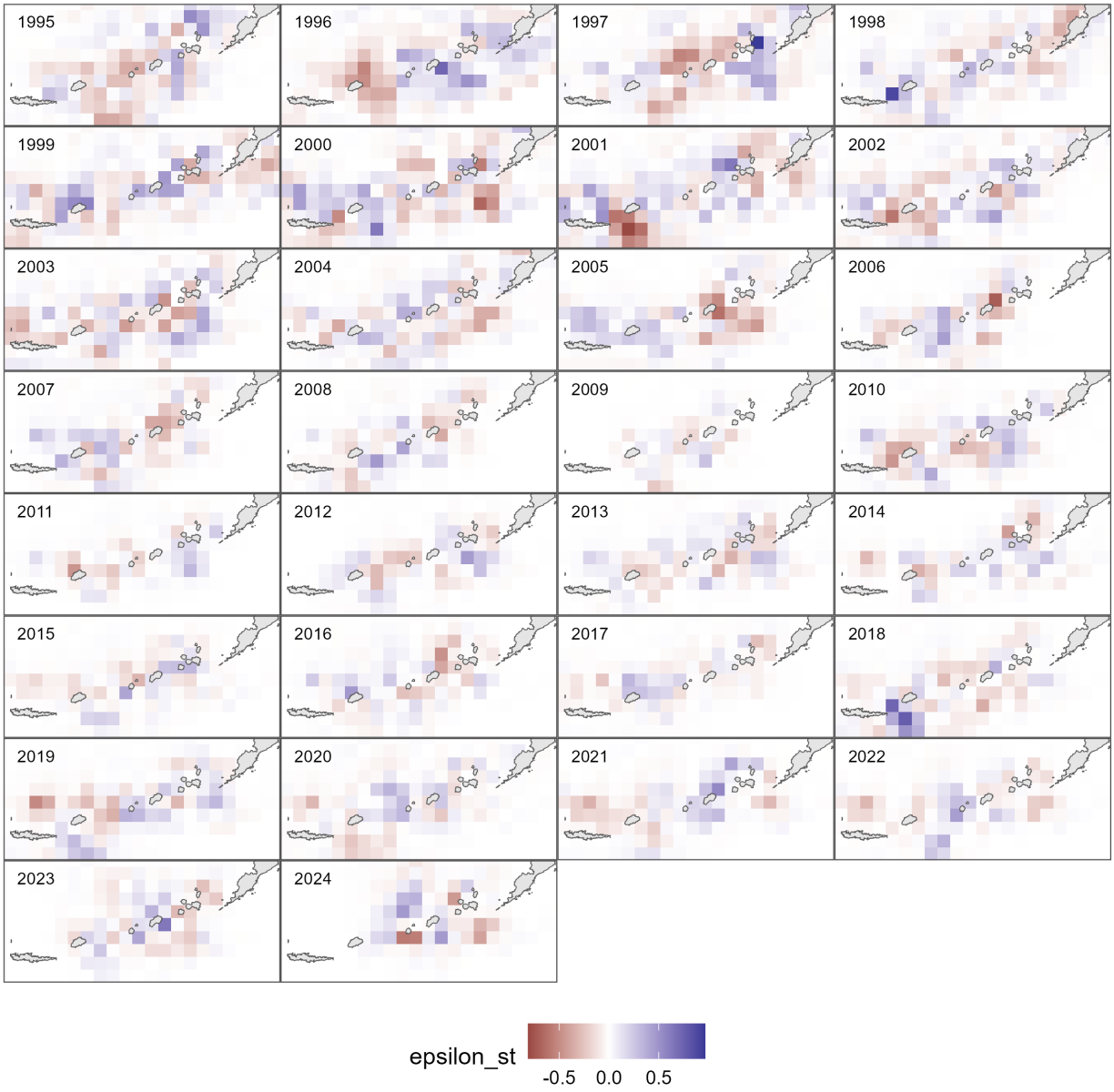

Figure 15: Spatiotemporal random effect for the model fit to the EAG.

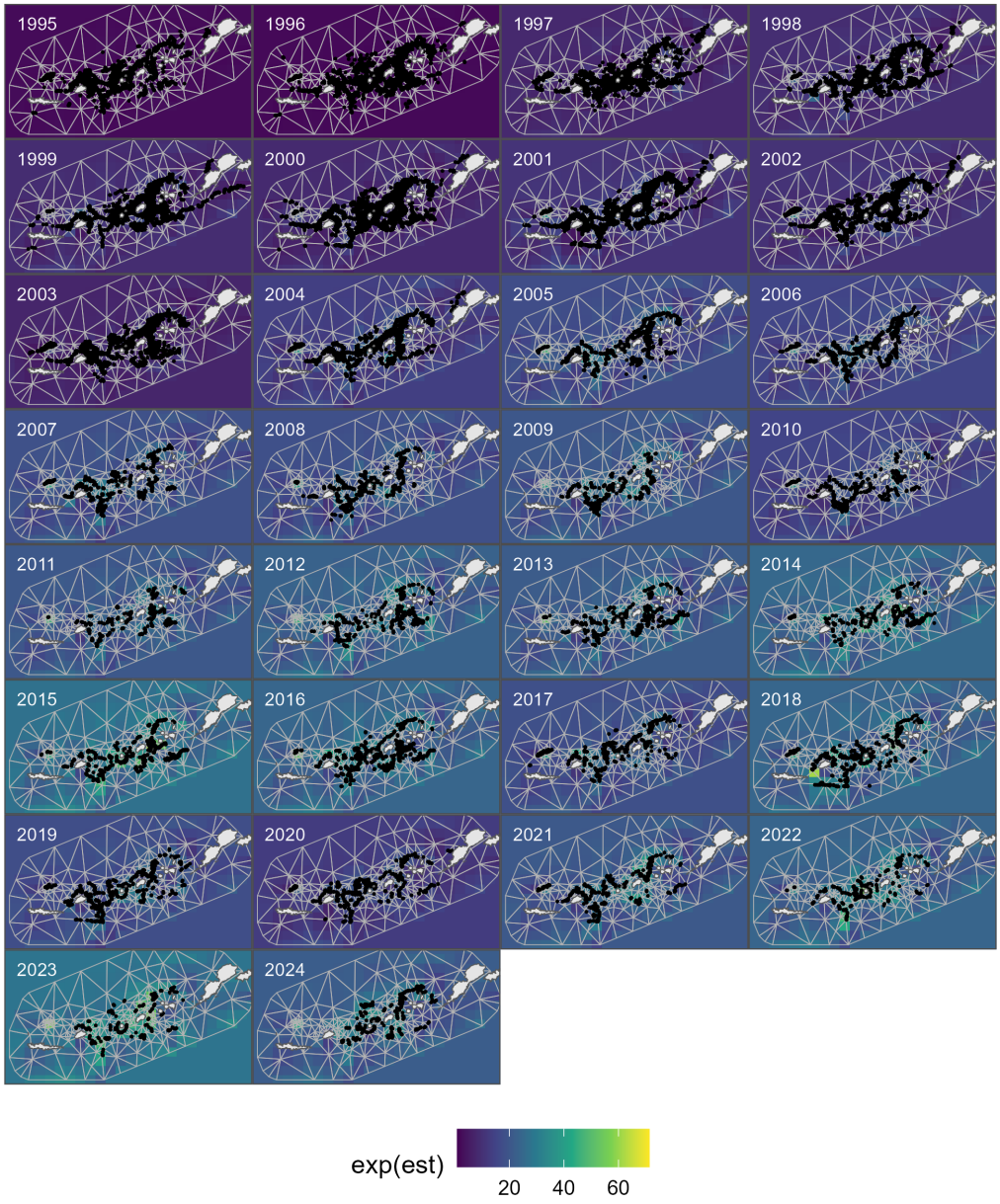

Figure 16: Predicted CPUE for the spatiotemporal model fit to the EAG.

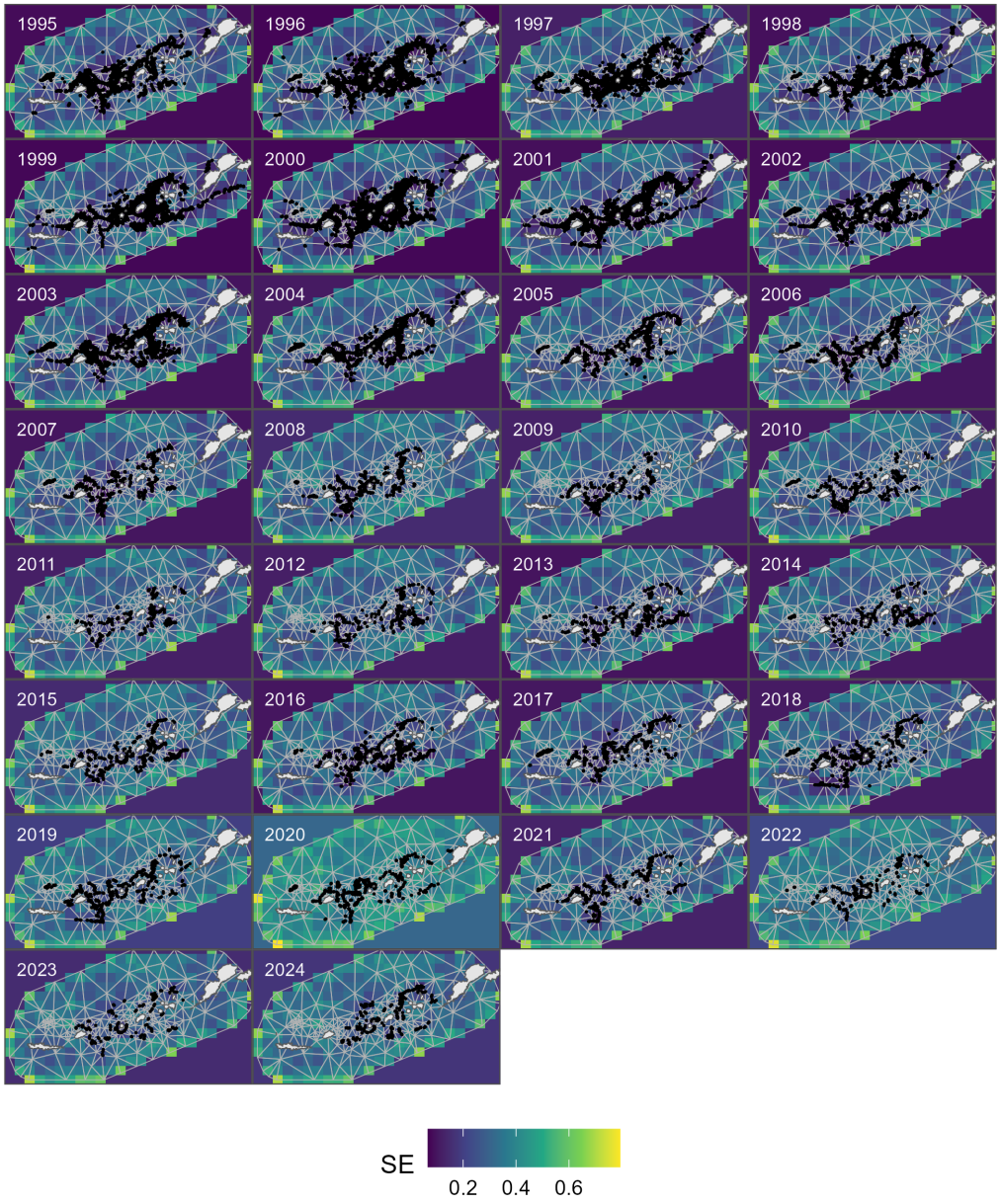

Figure 17: Standard error on predicted CPUE for the spatiotemporal model fit to the EAG.

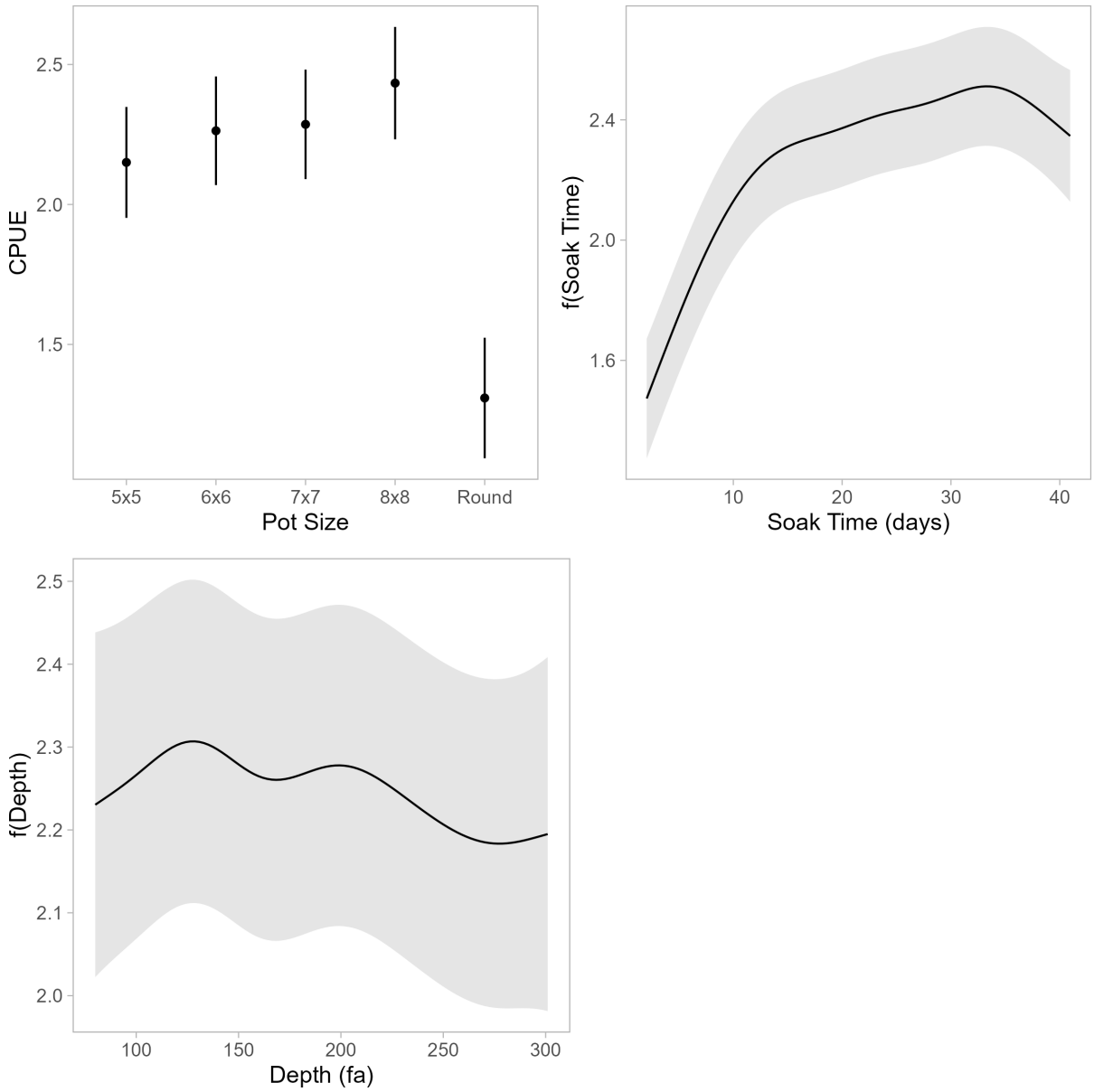

Figure 18: Marginal effects of gear type, soak time, and depth for the spatiotemporal model fit to the WAG.

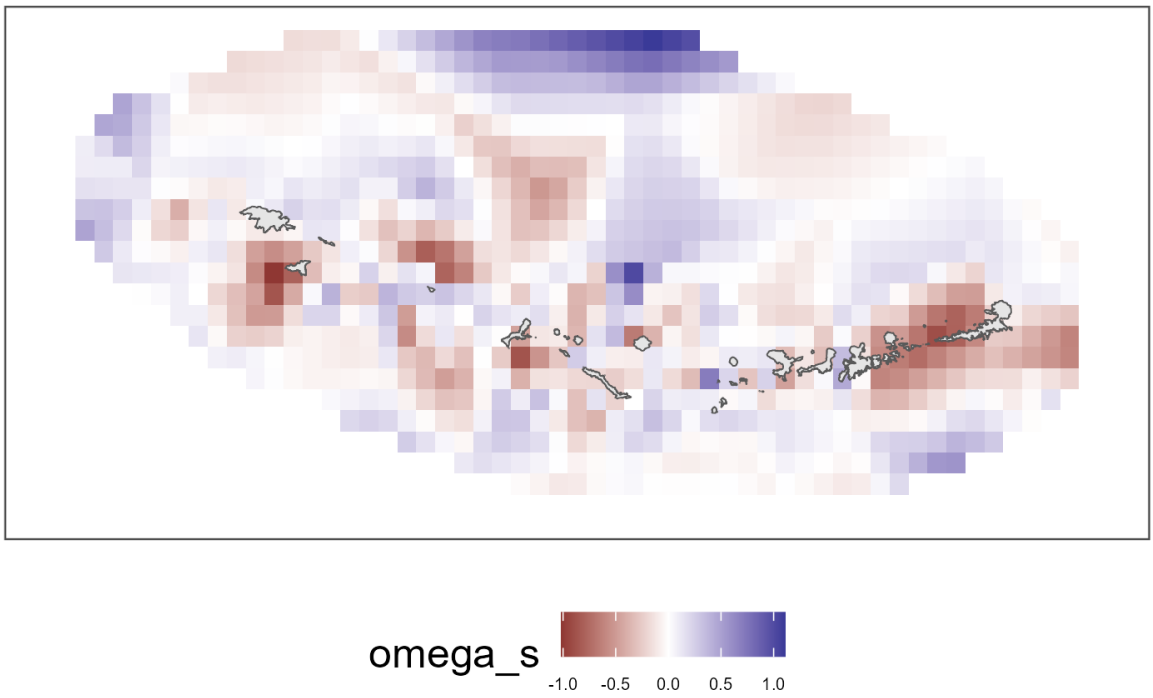

Figure 19: Spatial random effect for the spatiotemporal model fit to the WAG.

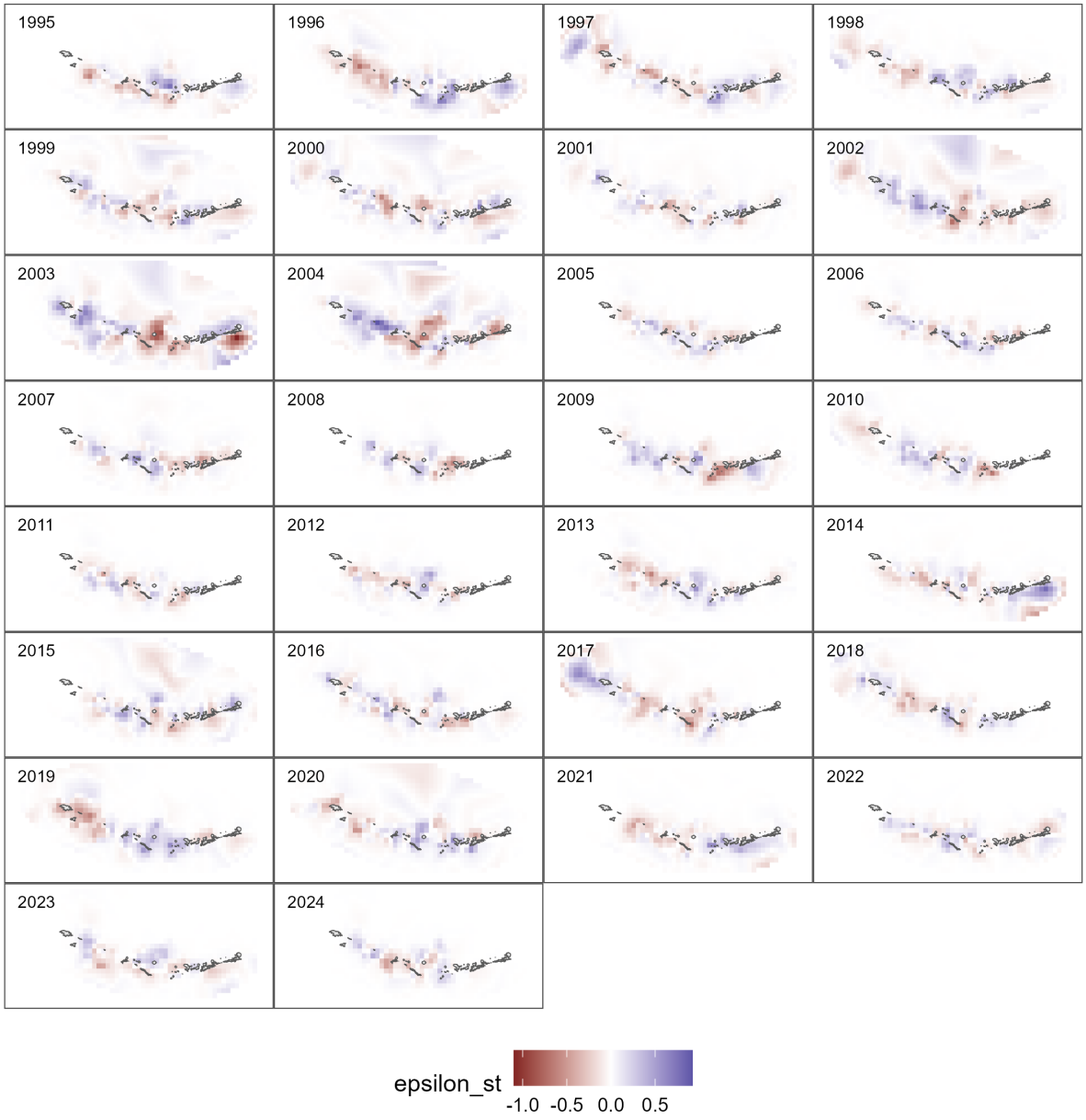

Figure 20: Spatiotemporal random effect for the model fit to the WAG.

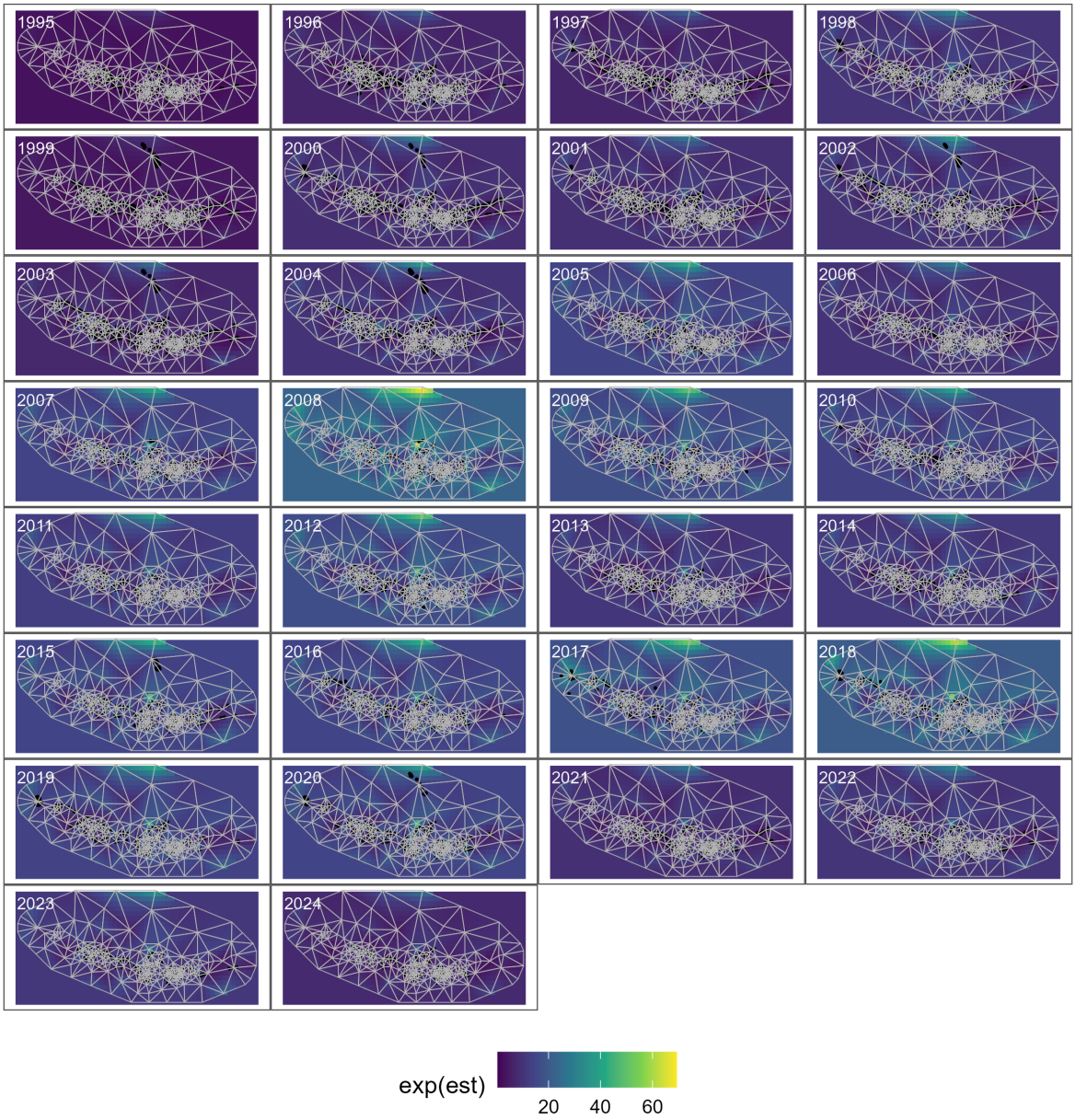

Figure 21: Predicted CPUE for the spatiotemporal model fit to the WAG.

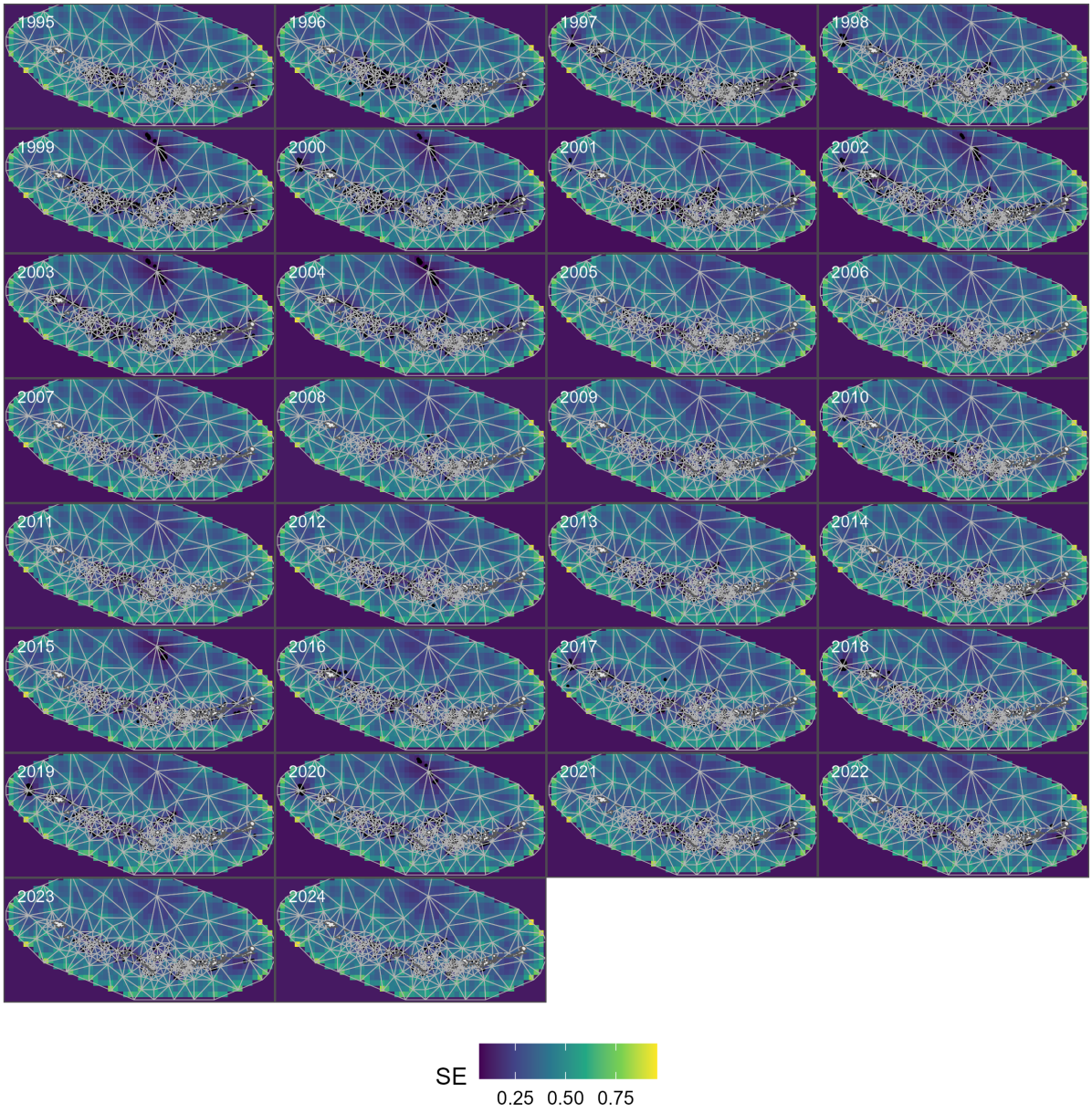

Figure 22: Standard error on predicted CPUE for the spatiotemporal model fit to the WAG.

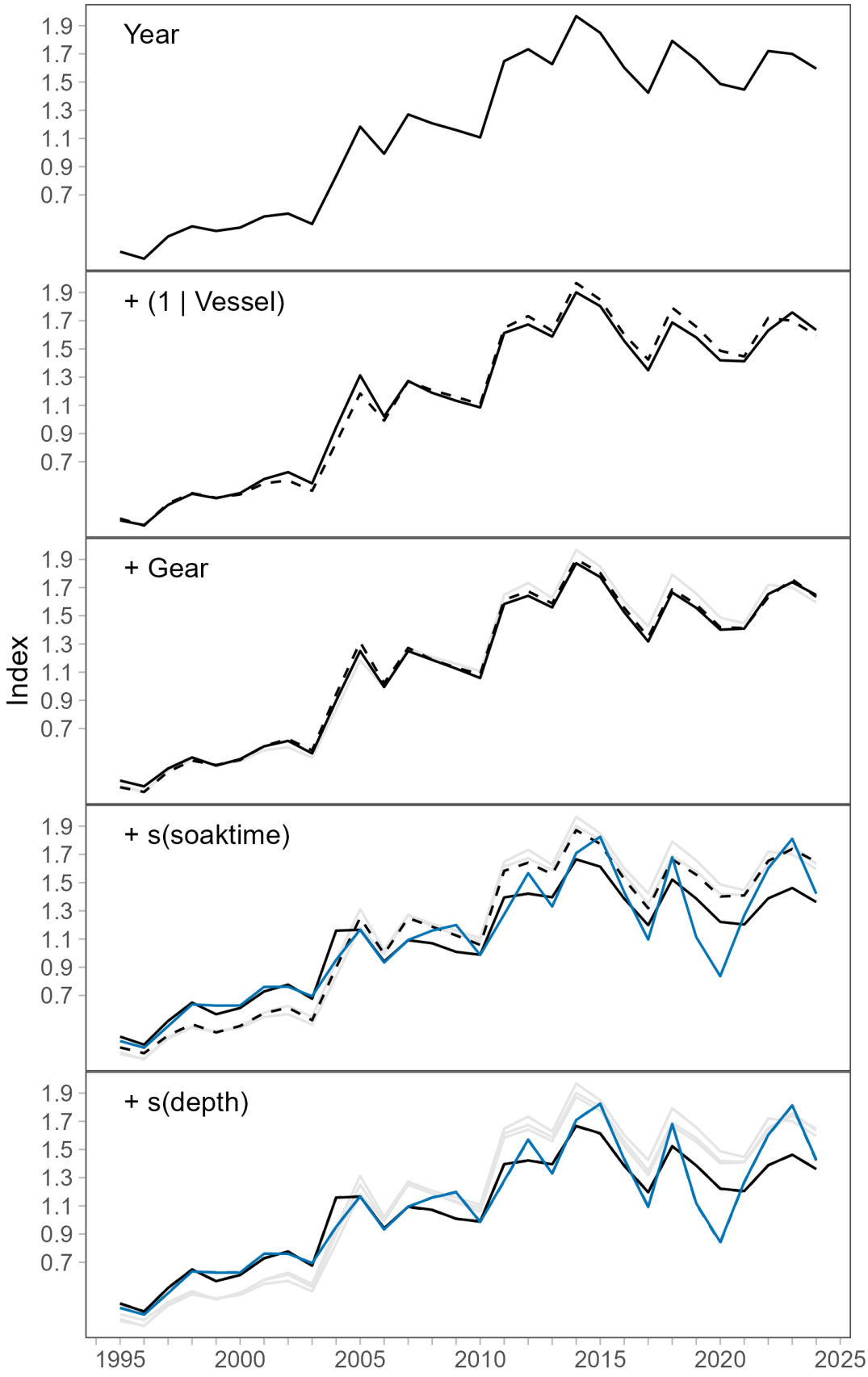

Figure 23: Step plot of CPUE index for the spatiotemporal model fit to the EAG. The model with the s(soak time):year interaction is in blue.

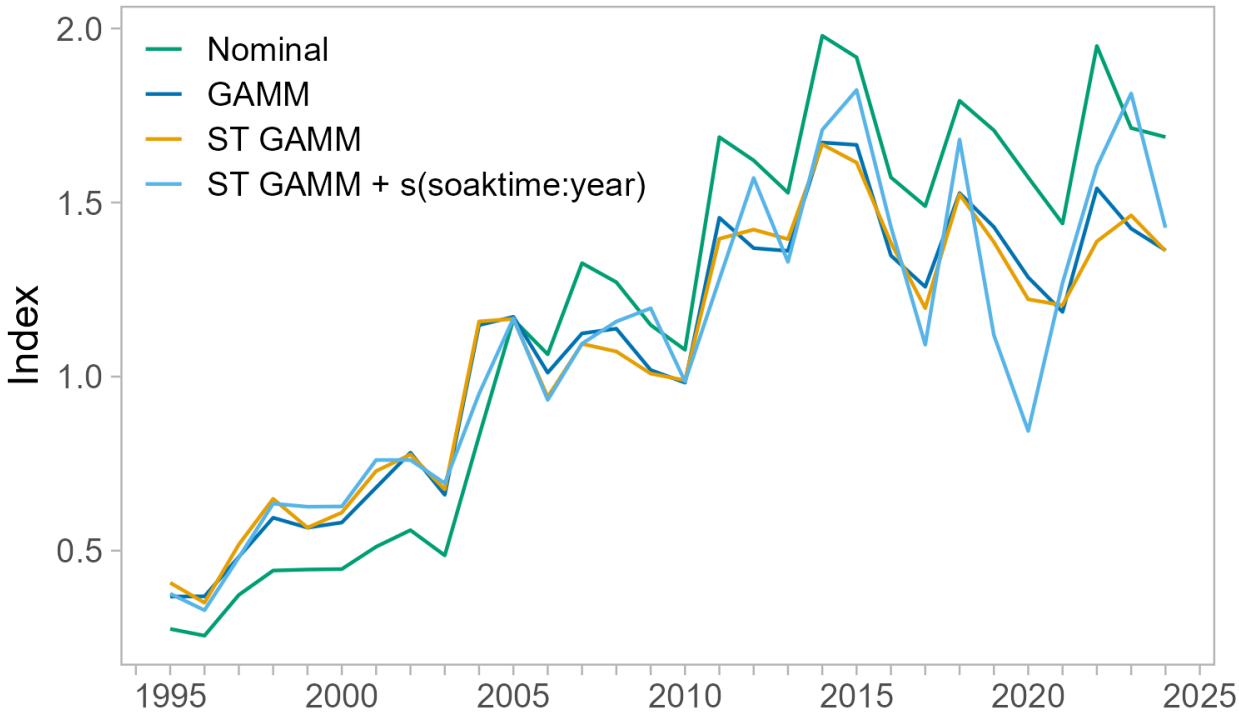

Figure 24: Comparison of nominal CPUE and standardized indices from a GAMM without spatial effects and the spatiotemporal model with the s(soak time):year interaction for the EAG.

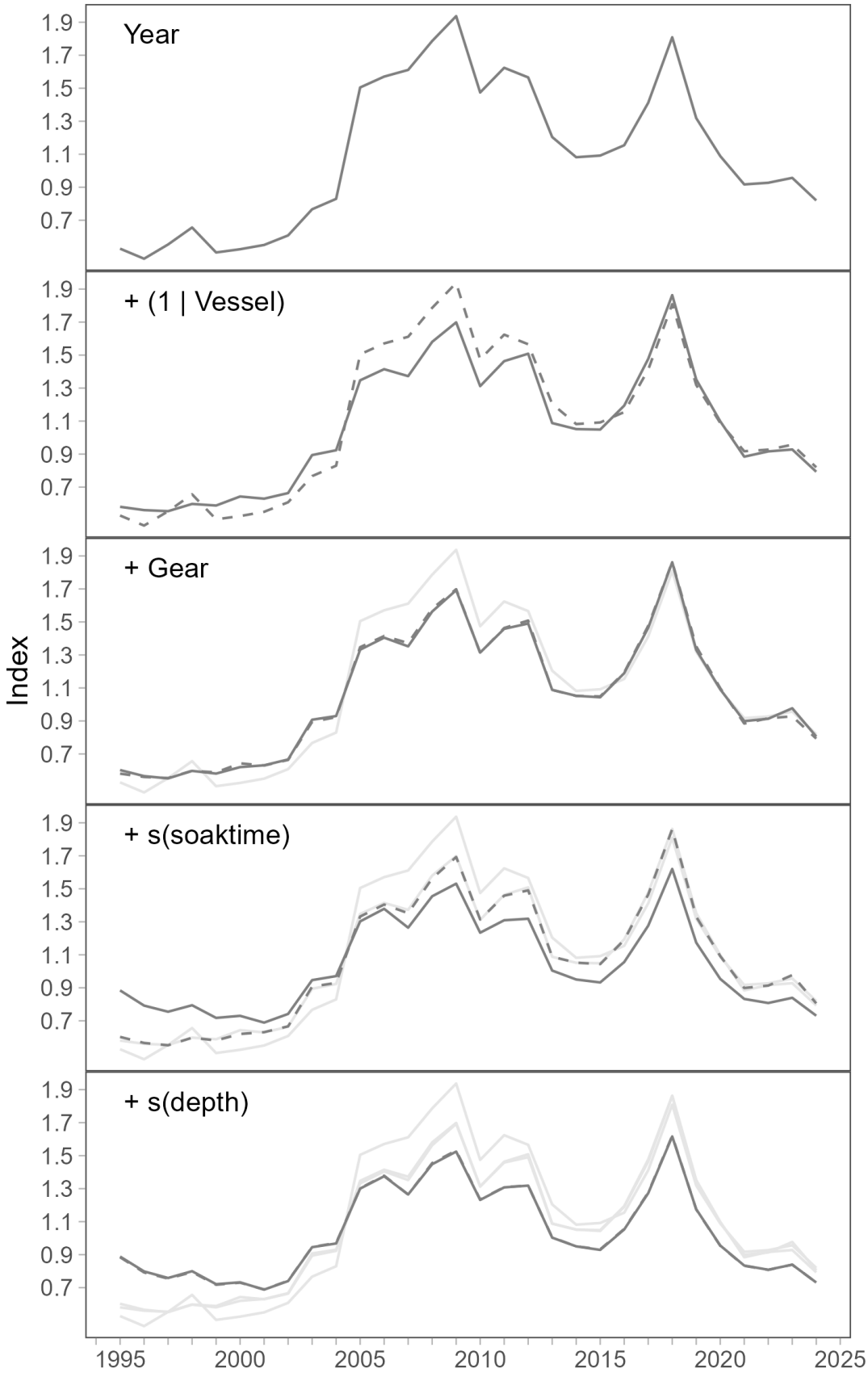

Figure 25: Step plot of CPUE index for the spatiotemporal model fit to the WAG. The model with the s(soak time):year interaction is in blue.

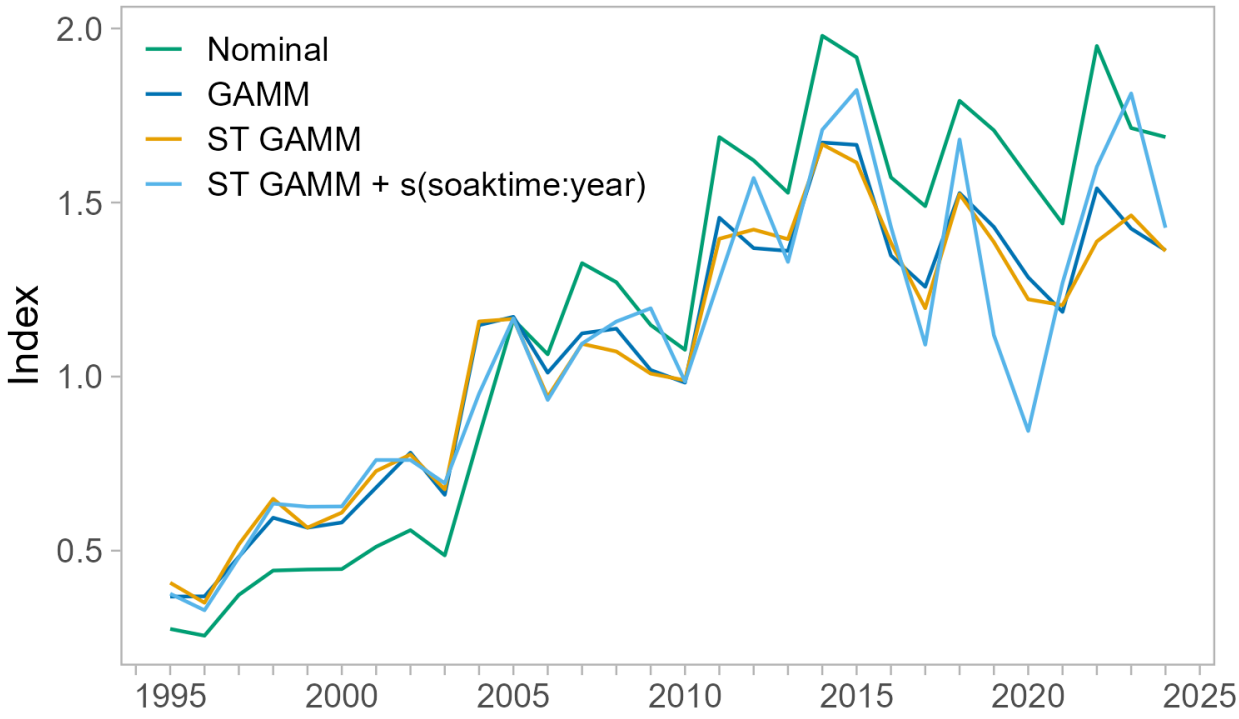

Figure 26: Comparison of nominal CPUE and standardized indices from a GAMM without spatial effects and the spatiotemporal model with the s(soak time):year interaction for the WAG.

Literature Cited

Anderson SC. 2025. sdmTMBextra: Extra Functions for Working with 'sdmTMB' Models_. R package version 0.0.4, commit 63f236912e12ce78b5a0529eedf1e11cb93d0a10, https://github.com/pbs-assess/sdmTMBextra.

Anderson, SC, EJ Ward, PA English, LAK Barnett, JT Thorson. 2024. sdmTMB: an R package for fast, flexible, and user-friendly generalized linear mixed effects models with spatial and spatiotemporal random fields. bioRxiv 2022.03.24.485545.

Bentley, N, TH Kendrick, PJ Starr, and PA Breen. 2012. Influence plots and metrics: tools for better understanding fisheries catch-per-unit-effort standardizations. ICES Journal of Marine Science, 69: 84-88.

Bishop, J, WN Venables, CM Dichmont, and DJ Sterling. 2008. Standardizing catch rates: is logbook information by itself enough? ICES Journal of Marine Science 65: 255-266.

Bozdogan, H. 1987. Model selection Akaike's information criterion (AIC): The general theory and its analytical extensions. Psychometrika 52: 345-370.

Lindgren F, H Rue, and J Lindström. 2011. An explicit link between Gaussian fields and Gaussian markov random fields: The stochastic partial differential equation approach. Journal of the Royal Statistical Society B 73: 423 - 498.

Hartig, F. 2020. DHARMa: Residual Diagnostics for Hierarchical (multi-Level / Mixed) Regression Models. https://CRAN.R-project.org/package=DHARMa.

Hijmans RJ, M Barbosa, A Ghosh, and A Mandel. 2025. geodata: Download Geographic Data. R package version 0.6-3, https://github.com/rspatial/geodata.

Hoyle SD, RA Campbell, ND Ducharme-Barth, A Grüss, BR Moore, JT Thorson, L Tremblay-Boyer, H Winker, S Zhou, MN Maunder. 2024. Catch per unit effort modelling for stock assessment: A summary of good practices. Fisheries Research 269: 106860.

Jackson, TM. 2024a. Aleutian Islands golden king crab stock assessment 2024. North Pacific Fishery Management Council, Anchorage, Alaska.

Maunder MN, JT Thorson, H Xu, R Oliveros-Ramos, SD Hoyle, L Tremblay-Boyer, HH Lee, M Kai, SK Chang, T Kitakado, CM Albertsen, CV Minte_vera, CE Lennert-Cody, AM Aires-da-Silva, and KR Piner. 2020. The need for spatio-temporal modeling to determine catch-per-unit effort based indices of abundance and associated composition data for inclusion in stock assessment models. Fisheries Research 229: 105594.

Redlands, CESRI. (2011). ArcGIS Desktop: Release 10.

Siddeek, MSM, J Zheng, and D Pengilly. 2016. Standardizing CPUE from the Aleutian Islands golden king crab observer data. Pages 97–116 in TJ Quinn II, JL Armstrong, MR Baker, J Heifetz, and D Witherell (eds.), Assessing and Managing Data-Limited Fish Stocks. Alaska Sea Grant, University of Alaska Fairbanks, Alaska.

Siddeek, MSM, T Jackson, B Daly, C Siddon, MJ Westphal, and L Hulbert. 2023. Aleutian Islands golden king crab model scenarios for May 2023 assessment. North Pacific Fishery Management Council, Anchorage, Alaska.

Wood, S. 2004. Stable and efficient multiple smoothing parameter estimation for generalized additive models. Journal of the American Statistical Association 99: 673-686.

Zimmermann, M, MM Prescott, and CN Rooper. 2013. Smooth Sheet Bathymetry of the Aleutian Islands. U.S. Dep. Commer., NOAA Tech. Memo. NMFS-AFSC-250, 43p.